



# Adaptive methods for semi-linear elliptic equations with critical exponents and interior singularities

C.J. Budd<sup>a,\*</sup>, A.R. Humphries<sup>b</sup>

<sup>a</sup> School of Mathematics, University of Bath, Claverton Down, Bath BA2 7AY, UK

<sup>b</sup> Centre for Mathematical Analysis and its Applications, School of Mathematical Sciences, University of Sussex, Brighton BN1 9QH, UK

---

## Abstract

We consider the effectiveness of adaptive finite element methods for finding the finite element solutions of the parametrised semi-linear elliptic equation  $\Delta u + \lambda u + u^5 = 0$ ,  $u > 0$ , where  $u \in C^2(\Omega)$ , for a domain  $\Omega \subset \mathbb{R}^3$  and  $u = 0$  on the boundary of  $\Omega$ . This equation is important in analysis and it is known that there is a value  $\lambda_0 > 0$  such that no solutions exist for  $\lambda < \lambda_0$  and a singularity forms as  $\lambda \rightarrow \lambda_0$ . Furthermore the linear operator  $L$  defined by  $L\phi = \Delta\phi + \lambda\phi + 5u^4\phi$  has a singular inverse in this limit. We demonstrate that conventional adaptive methods (using both static and dynamic regridding) based on usual error estimates fail to give accurate solutions and indeed admit spurious solutions of the differential equation when  $\lambda < \lambda_0$ . This is directly due to the lack of invertibility of the operator  $L$ . In contrast we show that error estimates which take this into account can give answers to any prescribed tolerance. © 1998 Elsevier Science B.V.

*Keywords:* Semi-linear elliptic partial differential equation; Adaptive finite element methods; Critical exponent; Spurious solutions; Asymptotic error estimates

---

## 1. Introduction

### 1.1. Preliminaries

An interesting class of parametrised semi-linear elliptic partial differential equations with solutions which develop isolated singularities as the parameter varies, is given by the system

$$\begin{cases} \Delta u + \lambda u + u^5 = 0 & \text{on } \Omega \subset \mathbb{R}^3, \\ u > 0 & \text{in } \Omega, \\ u = 0 & \text{on } \partial\Omega, \end{cases} \quad (1.1)$$

---

\* Corresponding author. E-mail: cjb@maths.bath.ac.uk.

where  $\Omega$  is a bounded domain in  $\mathbb{R}^3$ . This and related problems play an important role in analysis, where the nonlinearity  $u^5$  is said to grow at a *critical* rate [3,4]. It lies on the borderline of problems which can be solved by using the calculus of variations and also plays a role in the study of manifolds with prescribed curvature [15] and investigations of stellar structure [9]. See also a discussion in [2] for its links with topology.

In general it is known that there is a *branch* of solutions  $(\lambda, u) \in \mathbb{R} \times C^2(\Omega)$  for  $\lambda_0 < \lambda < \lambda_1$ , where  $\lambda_1$  is the principle eigenvalue for the Laplacian on the domain  $\Omega$ . However, for certain domains it is known that a singularity develops as  $\lambda$  approaches a critical value of  $\lambda_0 > 0$  from above. If  $\lambda < \lambda_0$  then the problem (1.1) has *no* nontrivial solution. In this case we have that as  $\lambda \rightarrow \lambda_0^+$

$$\|u\|_\infty \rightarrow \infty \quad \text{and} \quad \|u\|_{H_0^1} \rightarrow 3^{3/4}\pi/2. \quad (1.2)$$

Here  $H_0^1(\Omega)$  is the usual Sobolev space of functions with square integrable first derivative. Observe that the behaviour in the two norms is quite different. An important question of interest to analysts, and the underlying motivation of our calculations, is an accurate identification of  $\lambda_0$  for a general domain.

If a non-adaptive finite element method with a fixed mesh is used to solve this problem then it is known [7,8,12,14] that there is a corresponding (discrete) solution branch  $(\lambda, U) \in \mathbb{R} \times H_0^1(\Omega)$  such that  $U$  exists for *all* values of  $\lambda < \lambda_1$  and that  $\|U\|_\infty$  is bounded for all such values. This behaviour is in stark contrast to that of the continuous problem and should hopefully be improved by using an adaptive procedure. To calculate the value of  $\lambda_0$  accurately such a procedure should fulfill the following requirements:

- (1) For all  $\lambda$  such that a solution exists, it should efficiently calculate  $u$  to a prescribed tolerance.
- (2) It should avoid calculating *spurious* solutions. That is, solutions of the numerical method which exist (for example, when  $\lambda < \lambda_0$ ) when the underlying problem has *no* solution.

A difficulty which arises when using standard adaptive procedures (for example, those described in [1,11]) to solve this problem, is that not only does  $u$  become unbounded in the maximum norm as  $\lambda$  approaches  $\lambda_0$  but it is also known [6] that the linear operator  $L$  associated with (1.1) and defined by

$$L\phi = \Delta\phi + \lambda\phi + 5u^4\phi, \quad \phi = 0 \quad \text{on} \quad \partial\Omega \quad (1.3)$$

has an inverse  $L^{-1}$  which is *unbounded* in the  $L_\infty$  operator norm in this limit. Many existing adaptive procedures are based upon error estimates which make the implicit assumption that  $L^{-1}$  has a bounded norm. These estimates are unreliable for problem (1.1) and adaptive methods based upon them are not accurate and admit spurious solutions and we give some examples of calculations to demonstrate this.

In this paper we construct an adaptive procedure (based upon piecewise linear finite elements) which uses an estimate for the norm of  $L^{-1}$  and as a result employs a local error estimate for the discrete solution of (1.1) proportional to  $h^2u^8$  (where  $h$  is the local mesh size). We demonstrate that this is both accurate and does not admit spurious solutions.

A series of numerical calculations are presented to corroborate these results. To concentrate upon the issue of finding the correct error estimate, these calculations are made for the simplest case of finding a radially symmetric solution on the sphere (for which adaption need only be done in one dimension). They show that the estimate described above is reliable, and can in principle be used in a calculation over a much more general domain.

An important conclusion from this work is that when using an adaptive procedure to solve a nonlinear problem, it is essential to make a good estimate for the inverse of the linearisation of the operator,

otherwise the adaptive procedure will not necessarily offer much improvement over a non-adaptive method.

The layout of the remainder of this paper is as follows. In Section 2 we present some preliminary estimates for the solution of (1.1), in Section 3 we examine the performance of the static regridding locally uniform grid refinement method (LUGR) described in [1,16,17]. We show that standard error estimates (based upon curvature) are applied then they fail to give good results but if a revised method incorporating estimates of  $L^{-1}$  is used, then good performance is observed. In Section 4 we examine the performance of adaptive methods which move the mesh points and show that this is similar to that of those static regridding methods which do not allow for the growth in  $\|L^{-1}\|_{\infty}$ . Finally, in Section 5 we draw some conclusions from this work.

## 2. Preliminary results

### 2.1. The nature of the singularity

Suppose that we define

$$\|u\|_{\infty} = \gamma \quad (2.1)$$

so that  $\gamma \rightarrow \infty$  as  $\lambda \rightarrow \lambda_0$ . By using formal asymptotic methods [6] it is conjectured that for general star-shaped domains, the function  $u(\mathbf{x})$  forms a singularity at the point  $\mathbf{x}_0$  such that in the limit as  $\lambda \rightarrow \lambda_0$

$$u(\mathbf{x}) \approx w_{\gamma}(\mathbf{x}) \equiv \frac{\gamma}{(1 + \gamma^4 |\mathbf{x} - \mathbf{x}_0|^2/3)^{1/2}}. \quad (2.2)$$

Thus  $u$  has a peak of height  $\gamma$  and width of order  $1/\gamma^2$ . The numerical procedure needs to resolve this structure. Observe also that  $u(\mathbf{x})$  is approximately radially symmetric close to  $\mathbf{x}_0$ . In Fig. 1 we present a cross section of a numerical solution of (1.1) together with a contour plot to give an indication of the form of the singularity. Here  $\Omega$  is a cube of side 1 and  $\lambda = 7.5045$  (see [8] where it is conjectured that this is the value of  $\lambda_0$  for this domain). For this calculation piecewise linear basis functions are used on a regular cuboid mesh.

### 2.2. The numerical scheme

A finite element scheme on a uniform mesh for the solution of (1.1), together with an error analysis, has been presented in [7] for the case of  $\Omega$  the sphere and in [8] for  $\Omega$  a cuboid. In this paper we mainly look at calculations of radially symmetric solutions on the sphere as this greatly simplifies the implementation of the method. However, as the singularity has a high degree of radial symmetry, the error estimates and certain other issues related to the computation are very similar to the more general case. The restriction to the sphere allows us to compare the performance of different methods without encountering the book-keeping and related difficulties associated with the more general method. We define two bilinear forms by

$$a(u, v) = \int_{\Omega} \nabla u \nabla v \, d\Omega \quad \text{and} \quad \langle u, v \rangle = \int_{\Omega} uv \, d\Omega.$$

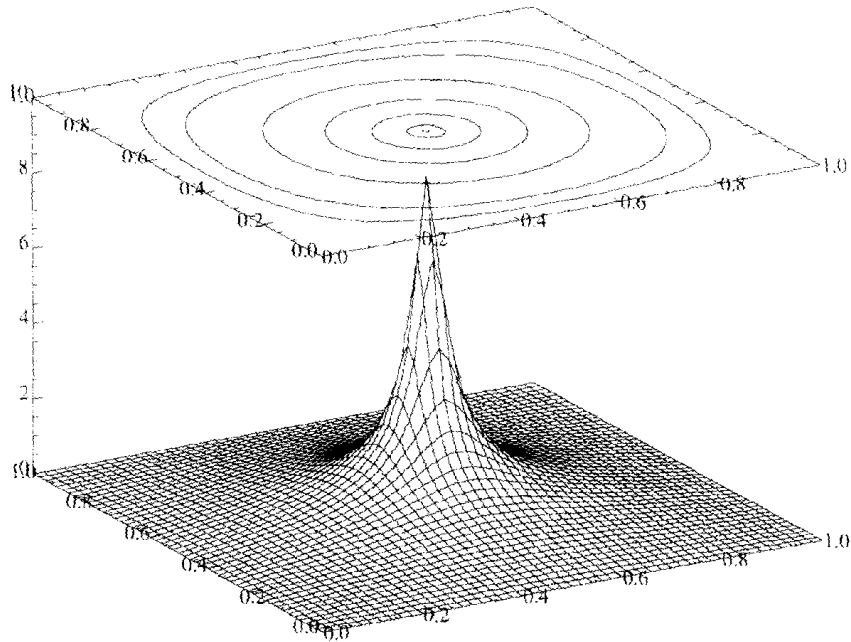


Fig. 1. A calculation of  $U_h$  in the unit cube with piecewise linear basis functions on a mesh with  $h = 1/100$  and  $\lambda = 7.5045$ . A cross-section is shown through the plane  $z = 0$  together with a contour plot, which shows the radial symmetry of the solution in the centre of the domain.

Now take  $\Omega$  to be the unit sphere and define a series of points  $r_i \in [0, 1]$  such that  $r_0 = 0$ ,  $r_i < r_{i+1}$ ,  $r_N = 1$  and  $r_{i+1} - r_i = h_i$ . Finally, define basis functions  $\phi_i(\mathbf{x})$  if  $0 < i < N$  by

$$\phi_i(\mathbf{x}) = \frac{|\mathbf{x}| - r_{i-1}}{r_i - r_{i-1}} \quad \text{if } r_{i-1} < |\mathbf{x}| < r_i, \quad (2.3)$$

$$\phi_i(\mathbf{x}) = \frac{r_{i+1} - |\mathbf{x}|}{r_{i+1} - r_i} \quad \text{if } r_i < |\mathbf{x}| < r_{i+1}, \quad (2.4)$$

$\phi_i(\mathbf{x}) = 0$  otherwise. If  $i = 0$ , then  $\phi_0(\mathbf{x})$  is defined by (2.4) only. Set  $S \subset H_0^1(\Omega)$  to be the span of these basis functions. The finite element approximation  $U$  to  $u$  is then the nontrivial function in  $S$  satisfying

$$-a(U, \phi_i) + \langle \lambda U + U^5, \phi_i \rangle = 0 \quad \forall i. \quad (2.5)$$

If the values of  $r_i$  are fixed then it is shown in [14] that the finite element solution so constructed is a differentiable function of  $\lambda$  and exists both for  $\lambda > \lambda_0$  when an underlying solution of (1.1) exists and for  $\lambda \leq \lambda_0$  when it does not. We label these two solutions *convergent* and *spurious*, respectively. In Fig. 2 we present a comparison of  $\|u\|_\infty$  and  $\|U\|_\infty$  as functions of  $\lambda$  for the case of a uniform mesh with  $h_i \equiv h = 1/128$ .

When  $\lambda > \lambda_0$  then  $U$  converges to  $u$  under mesh refinement. A general theory for the convergence of discrete approximations to solutions of a semi-linear elliptic partial differential equation for a uniform

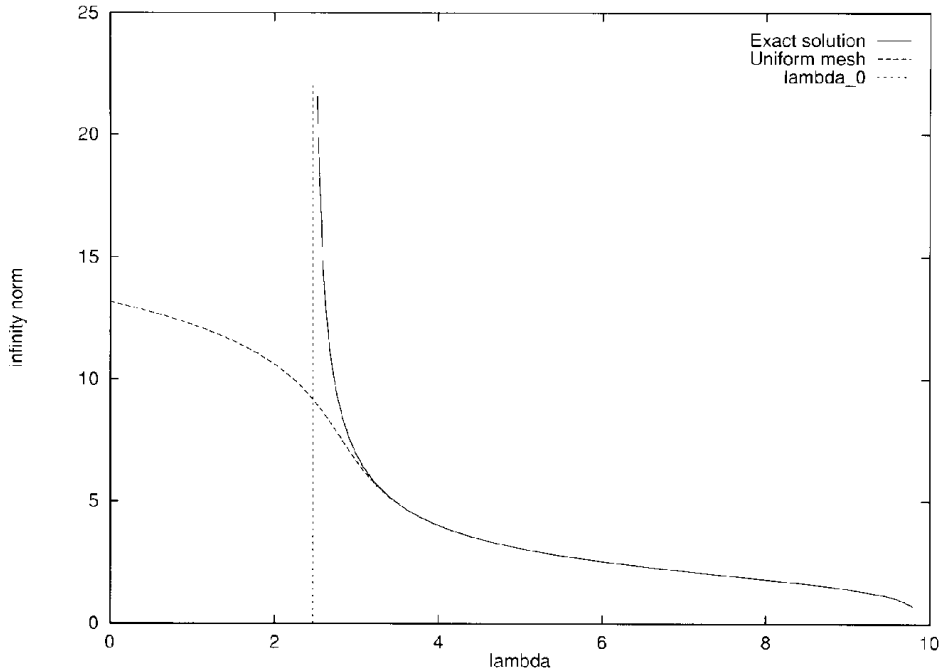


Fig. 2. A bifurcation diagram comparing the infinity norm of the true solution of (1.1) in the unit sphere with a discrete finite element solution with 128 elements. The value of  $\lambda_0 = \pi^2/4$  is indicated.

mesh. has been developed by several authors, for example [5,10,13]. In particular, if the mesh has size  $h$  and the corresponding discrete solution is  $U_h$  it is known that as  $h \rightarrow 0$  then

$$\|u - U_h\|_\infty < Ch^2 \log(1/h) \|L^{-1}\|_\infty \|\Delta u\|_\infty, \tag{2.6}$$

where the constant  $C$  does not depend upon  $u$  and  $L$  is the operator defined in (1.3). In fact this error estimate applies both for the basis functions described above and also for the case of piecewise linear basis functions defined on cubes or trapezia in more general domains. It is significant that in this estimate there are two contributions namely  $\|L^{-1}\|_\infty$  and  $\|\Delta u\|_\infty = \|\lambda u + u^5\|_\infty \approx \|u\|_\infty^5$  which both become large as  $\lambda \rightarrow \lambda_0$ .

In [7,8] a more precise error estimate has been derived by using formal asymptotic methods which are sharp for those values of  $\lambda$  for which  $u$  is large. In particular we have that as  $h \rightarrow 0$ , there are constants  $A$  and  $B$  such that

$$\|L^{-1}\|_\infty \approx A \|u\|_\infty^4 \quad \text{and} \quad \| \|u\|_\infty - \|U_h\|_\infty \| \approx Bh^2 \|u\|_\infty^9. \tag{2.7}$$

The constant  $B$  depends upon the elements used. For the basis functions in (2.3)  $B = 1.907 \times 10^{-4}$  and for trilinear functions on cubes  $B = 1.23 \times 10^{-4}$ . (Similar estimates can also be obtained for higher order elements.) The estimate (2.7) is only descriptive for very small values of  $h$ . An error estimate which applies for a much larger values can also be obtained asymptotically and takes the form

$$\|u\|_\infty \approx \frac{\|U_h\|_\infty}{(1 - 2Bh^2 \|U_h\|_\infty^8)^{1/2}}. \tag{2.8}$$

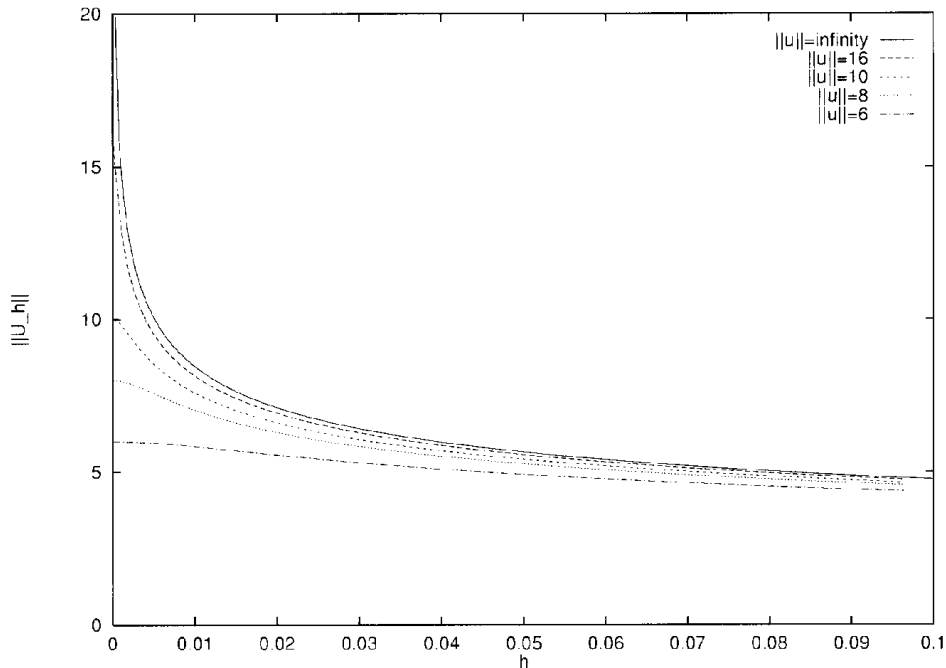


Fig. 3. The value of  $\|U_h\|$  as a function of  $h$  in the cases of  $\|u\|_\infty = 6, 8, 10, 16, \infty$ .

If  $\lambda \leq \lambda_0$  then  $U_h$  is spurious and does not converge to a function  $u$  under mesh refinement. In contrast  $\|U_h\|_\infty$  grows without bound, whereas  $\|U_h\|_{H_0^1}$  remains bounded. If we define  $U_0 \equiv U_h$  at  $\lambda = \lambda_0$  we have

$$\|U_0\|_\infty \approx (2B)^{-1/8} h^{-1/4} \quad \text{and} \quad \|U_0\|_{H_0^1} \approx 3^{3/4} \pi/2. \quad (2.9)$$

The estimate (2.9) can be obtained from (2.8) by putting  $\|u\|_\infty = \infty$ . The rate of growth of  $\|U_0\|_\infty$  as a function of  $h$  is very slow, and it is hard to tell under mesh refinement whether we are computing a convergent or a spurious solution. To emphasise this we present in Fig. 3, a series of graphs showing how  $\|U_h\|_\infty$  behaves as a function of  $h$ . In these graphs we take a series of values of  $\|u\|_\infty = 6, 8, 10, 16$  and  $\infty$  in (2.8) and solve for  $\|U_h\|_\infty$  as  $h$  decreases from 0.1 to 0. From this graph we can see both the convergent behaviour for very small  $h$  and also the apparent growth in both the convergent and the spurious solutions as  $h$  decreases through larger values. For  $h > 0.4$  the convergent and spurious solutions are very difficult to distinguish. This shows how difficult it is to calculate  $\lambda_0$  on a uniform mesh and why an adaptive procedure is required.

### 3. Adaptive strategies using locally uniform grid refinement (LUGR)

#### 3.1. Derivation of the method

As remarked earlier, an effective adaptive strategy should compute the convergent solutions accurately when  $\lambda > \lambda_0$  and should reject spurious solutions when  $\lambda < \lambda_0$ . As a first algorithm we

consider the static regridding (LUGR) methods proposed by Verwer and his coworkers [1,16,17]. These methods were originally developed to find finite difference solutions of time-dependent problems but similar principles apply for finding finite element solutions of parameter-dependent steady problems. The basic approach is as follows.

1. Start with a solution of (2.5) and a uniform mesh at some value of  $\lambda$ .
2. Reduce  $\lambda$  to  $\lambda - \Delta\lambda$  and compute a new solution of (2.5) on the mesh used in Step 1.
3. At each mesh point  $i$  compute an estimate  $M(U_i)$  for the relative solution error.
4. If  $M > \text{TOL}$  then flag the element.
5. Define a neighbourhood of  $I_i$  elements around the flagged element.
6. Refine (bisect) all the flagged elements and the  $I_i$  neighbours of these elements.
7. Recompute the solution on the new mesh.
8. Repeat from Step 3 until  $M < \text{TOL}$  on each element.
9. Choose a suitable  $\Delta\lambda$  and repeat from Step 2 with the most recent mesh.

Crucial to the success of this method is the choice of the error monitor  $M$  and the number  $I_i$  of elements neighbouring the flagged element which are refined. If  $h_i$  is a measure of the size of the element then it is suggested in [1] that in a fully three dimensional calculation each of the 26 neighbours of a flagged element should be refined and a curvature monitor of the relative error should be used such that

$$M(U_i) = Dh_i^2 \frac{|\Delta U_i|}{|U_i|}, \quad (3.1)$$

where  $D$  is a user specified constant closely related to the required error tolerance. This is, in fact, an estimate of the relative local truncation error. From (2.6) we see that this is a reasonable estimate of the relative global solution error provided that the value of  $\|L^{-1}\|_\infty$  is *bounded* as  $\lambda \rightarrow \lambda_0$ . However, this is not the case for our problem leading to difficulties with a direct implementation of this method. From (1.1) it follows that, for large  $|U_i|$ , we can estimate  $|\Delta U_i|$  by  $|U_i^5|$ . The function  $M$  above then approximates  $M(U_i) = Dh_i^2 U_i^4$ . More generally we can consider the monitor

$$M(U_i) = Dh_i^2 U_i^q, \quad (3.2)$$

with  $q = 4$  corresponding to (3.1) and  $q = 0$  to using a uniform mesh. We now determine the value of  $q$  which leads both to the most accurate solution and is also effective in rejecting spurious solutions.

### 3.1.1. Accuracy

To make an estimate of the error we note that the smallest value of  $h_i$  will be given when  $U_i$  is largest (at the centre of the peak) and make the assumption that the error estimate in (2.7) can be applied taking  $h$  to be this value of  $h_i$ . (In [7] it is shown that this is reasonable provided that the mesh does not depart too greatly from uniformity close to the peak.) Making this assumption, taking  $M \approx \text{TOL}$ , applying (2.7) and eliminating  $h$  we then have that

$$\frac{\|u\|_\infty - \|U\|_\infty}{\|u\|_\infty} \approx \frac{B}{D} \text{TOL} \|u\|_\infty^{8-q}. \quad (3.3)$$

From this estimate we see that taking  $q = 4$  leads to an error estimate which *grows* as  $\|u\|_\infty^4$  as  $\lambda \rightarrow \lambda_0$ , preventing an accurate resolution of the solution. (Note that this rate of growth is proportional to  $\|L^{-1}\|_\infty$ .)

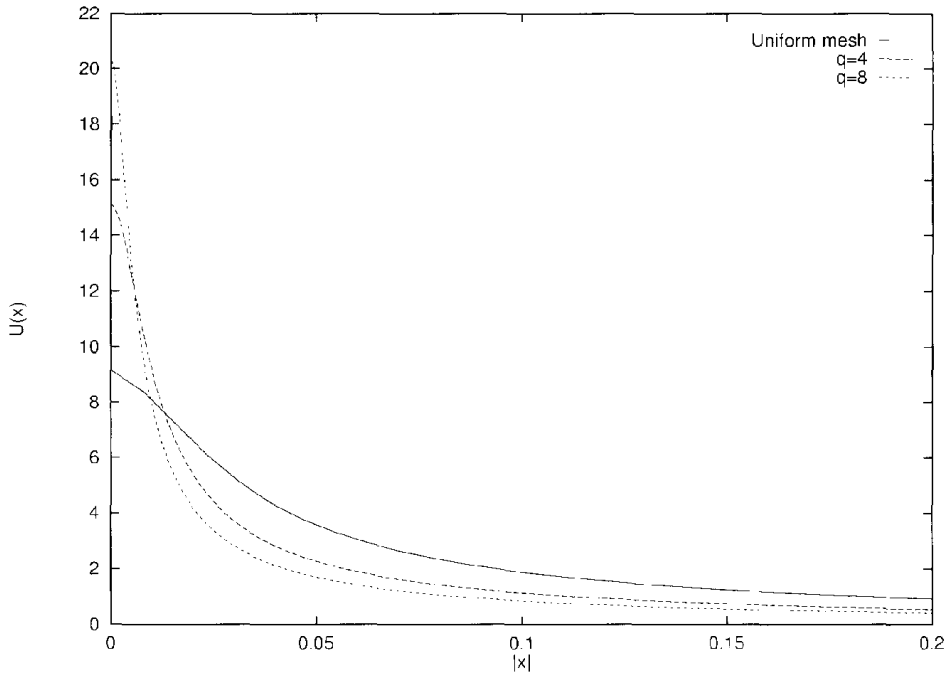


Fig. 4. Three profiles of computed solutions showing  $U_0$  in the two cases of a uniform mesh with 128 elements and an adaptive mesh with  $M = h_i^2 U_i^4$  and  $U$  for the optimal monitor with  $\lambda = 2.5244$ .

In contrast, if we take  $q = 8$  and set  $D = B$  then the error estimated above is bounded by TOL throughout the computation which is the first requirement for the adaptive method to be effective.

3.1.2. Rejection of spuriousity

Suppose now that  $\lambda = \lambda_0$ . We examine the spurious solution, which we again label as  $U_0$ . If we use a uniform mesh then from (2.9)  $\|U_0\|_\infty = (2B)^{-1/8} h^{-1/4}$ . As before, we assume that we can still use this estimate taking  $h$  to be the smallest value of  $h_i$  (see [7]). For such a value of  $h_i$  the application of the adaptive procedure implies that  $h_i^2 \|U_0\|_\infty \approx \text{TOL}$ . Eliminating  $h_i$  we have

$$\|U_0\|_\infty = (2BD^{-q} \text{TOL})^{-1/(8-q)}. \tag{3.4}$$

If  $q = 4$ , this result predicts that a spurious solution will exist with a finite norm given by

$$\|U_0\|_\infty = (2BD^{-4} \text{TOL})^{-1/4}. \tag{3.5}$$

When applying the adaptive routine with this value of  $q$  the grid is refined as  $\lambda$  is reduced but at  $\lambda_0$  a solution is still calculated and in fact a solution is determined for smaller values of  $\lambda$  as well. The implications of this result are rather worrying. The additional complexity of the adaptive algorithm has not prevented a false solution being computed. A profile of the corresponding solution for  $\text{TOL} = 0.1$  is presented in Fig. 4, and it is evident that this solution looks very believable. This makes a detection of its spurious nature even harder. Observe however, that as TOL becomes smaller, the value of  $\|U_0\|_\infty$  increases.

If  $q$  is increased from 0, the value of  $\|U_0\|_\infty$  increases and becomes infinite when  $q = 8$ . We deduce that no spurious solution exists when  $q = 8$ .

The optimal monitor of the relative error, both for accuracy and for rejecting spuriousity therefore appears to be

$$M = 2Bh_i^2U_i^8. \quad (3.6)$$

(A larger value of  $q$  will also be effective, but leads to more mesh refinement than is necessary.)

### 3.1.3. Choice of $I_i$

Before applying this method we need to make an estimate for the value  $I_i$  of the number of neighbours of the  $i$ th element that should be refined. Preliminary estimates using the monitor in (3.6) give poor values when only the immediate neighbours of the flagged elements are refined, in certain cases giving unstable solutions. Now, the major error will occur at the centre of the peak—and in the adaptive algorithm, the element at the centre is the first to be flagged. However, for an accurate solution all of the elements within the peak need to be refined. From (2.2) the width  $W$  of the peak is of order  $W = 1/\|u\|_\infty^2$ . Suppose that we assume, as before, that  $h_i^2\|u\|_\infty^q \approx 2B \text{ TOL}$  at the centre of the peak. We then have that

$$W/h_i \text{ is of order } \|u\|_\infty^{(q-4)/2} \text{ TOL}^{-1/2}. \quad (3.7)$$

This gives an estimate for the number of elements that need to be refined. If  $q = 4$  then approximately the same number of points are always placed within the peak independent of the maximum value of  $u$ . However, for the optimal value of  $q = 8$  this estimate is unbounded as  $\lambda \rightarrow \lambda_0$  which implies that we will not achieve a consistent accuracy with a *fixed* number of mesh points (unless we use  $p$ -refinement). As this number grows the implication is that  $I_i$  should also increase with  $\|u\|_\infty$ . In practice, when using the radially symmetric elements then taking the fixed, but large value of  $I_i = 64$  proved sufficient. (For the case of cuboid elements the additional geometrical complexity implies that the corresponding value of  $I_i$  will be much higher.)

## 3.2. Results

Although the algorithm can in principle be applied to calculations in a general domain, we restrict our attention to the sphere and the basis functions described above. In this case, refinement need only be applied to calculate the values of  $r_i$  which is a much simpler computational task than refining a cuboid or tetrahedral mesh. Furthermore, in this case the value of  $\lambda_0$  is known a-priori as  $\lambda_0 = \pi^2/4 = 2.4674011$  and an ‘exact’ radially symmetric solution  $u(\mathbf{x}) \equiv u(|\mathbf{x}|)$  can be constructed by using a shooting method. Knowing the exact solution we can compute an actual error ERR defined by

$$\text{ERR} = \frac{\|u\|_\infty - \|U\|_\infty}{\|u\|_\infty}.$$

For the first computation we take  $M$  as defined in (3.6),  $I_i = 64$ ,  $\text{TOL} = 0.1$  and start the computation at  $\lambda = 3.4$  with an initial uniform mesh of 32 elements. In this calculation we set  $\Delta\lambda = 0.2$  if  $\|u\|_\infty < 5$ , and  $25/\|u\|_\infty^3$  otherwise. Here  $N$  is the number of elements used in the computation and  $1/h_0$  is the inverse of the size of the smallest element. Table 1 shows clearly that the method is very effective in keeping the error in  $U$  within the required tolerance, and that re-meshing

Table 1

$\lambda$	$\ U\ _\infty$	$\ u\ _\infty$	ERR	$1/h_0$	$N$
3.4000	4.9625	5.1743	0.0409	32	32
3.1954	5.6586	5.8769	0.0371	64	64
3.0575	6.0743	6.5474	0.0722	64	64
2.9459	6.8870	7.2920	0.0555	128	128
2.8694	7.2706	7.9751	0.0883	128	128
2.8043	8.1991	8.7315	0.0610	256	193
2.7590	8.5722	9.4035	0.0884	256	193
2.7193	9.5830	10.1355	0.0545	512	258
2.6909	9.9640	10.7755	0.0753	512	258
2.6656	10.3104	11.4572	0.1001	512	258
2.6428	11.4877	12.1951	0.0580	1024	324
2.6263	11.8566	12.8250	0.0755	1024	324
2.6113	12.1977	13.4895	0.0958	1024	324
2.5975	13.4909	14.1984	0.0498	2048	390
2.5873	13.8664	14.7991	0.0630	2048	390
2.5780	14.2190	15.4241	0.0781	2048	390
2.5693	14.5494	16.0791	0.0951	2048	390
2.5612	16.0368	16.7710	0.0438	4096	457
2.5551	16.4111	17.3491	0.0541	4096	457
2.5494	16.7666	17.9452	0.0657	4096	457
2.5441	17.1035	18.5630	0.0786	4096	457
2.5391	17.4224	19.2066	0.0929	4096	457
2.5344	19.1918	19.8805	0.0346	8192	525
2.5309	19.5658	20.4330	0.0424	8192	525
2.5275	19.9237	20.9985	0.0512	8192	525
2.5244	20.2657	21.5792	0.0609	8192	525

occurs very close to the point for which  $\text{ERR} = 0.1$  showing that the estimated and actual errors are very close. The effectiveness of the method for this problem gives us confidence in applying it to problems for which  $\lambda_0$  is unknown although we see that the method has used a rather large number of mesh points to achieve this result.

For the second computation we take  $M = h_i^2 U_i^4$  (i.e.,  $q = 4$  in (3.2)) and compute  $\|U_0\|_\infty$  at  $\lambda_0$  for a range of values of TOL. This gives Table 2.

Table 2

TOL	$\ U_0\ _\infty$	$1/h_0$	$N$	$\text{TOL}^{1/4}\ U_0\ _\infty$
0.4	10.8110	256	130	8.597
0.2	12.7747	512	258	8.543
0.1	15.1501	512	325	8.519
0.05	18.0118	1024	391	8.517
0.025	21.4737	2048	460	8.539
0.0125	24.6468	4096	535	8.241

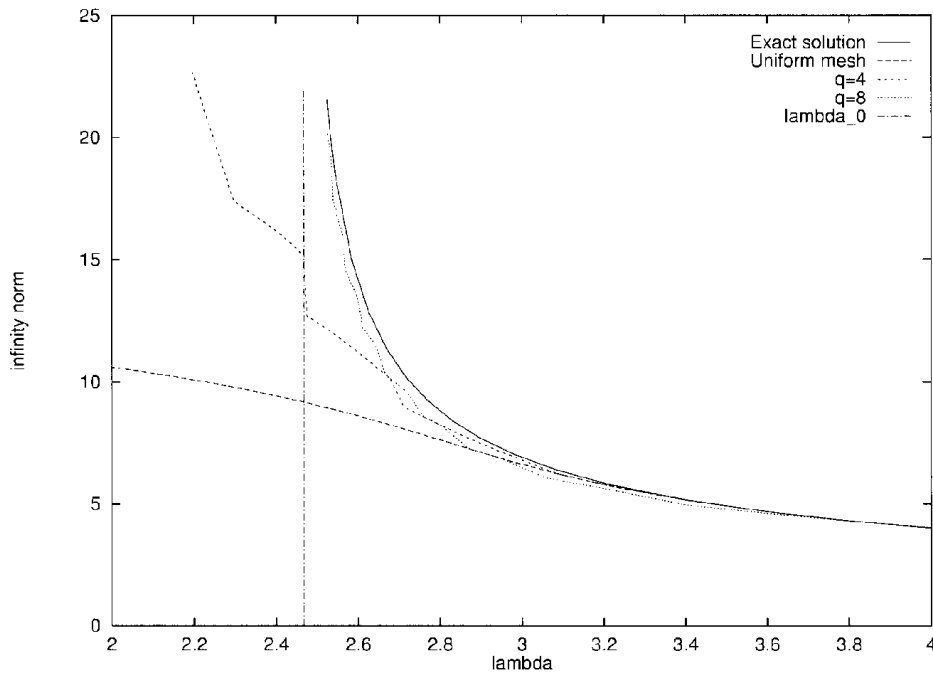


Fig. 5. A comparison of the true bifurcation diagram with the computed diagram using the three methods described in Fig. 4. The value of  $\lambda_0$  is also indicated.

From this table, it is fairly clear that  $\|U_0\|_\infty$  is indeed scaling at close to the predicted rate of  $\text{TOL}^{-1/4}$ .

In Fig. 4 we present the profile of the computed solutions  $U_0$  determined above when  $\text{TOL} = 0.1$  and compare it with the profile of  $U_0$  obtained with a uniform mesh with  $h = 1/128$  and also a solution computed using the optimal monitor (3.6) taking  $\lambda = 2.5244 > \lambda_0$ . In this figure we present the computed solution as a function of  $|\mathbf{x}|$  over the restricted range of  $0 \leq |\mathbf{x}| < 0.2$ . This range is chosen so that the profile of the peak can be seen clearly. Again, it is clear from this figure that all the profiles look quite plausible—even though two correspond to spurious solutions.

Finally, in Fig. 5 we present three bifurcation diagrams of the computed graph of  $(\lambda, \|U\|_\infty)$  for a uniform mesh with 128 elements and the two adaptive meshes described above. Note that all three

graphs are close to the exact bifurcation diagram if  $\lambda > 3$  but that they diverge markedly for smaller values. It is clear from this figure that whereas the bifurcation diagram for the uniform mesh is smooth, the curves obtained in the adaptive cases are not and show discontinuous changes in gradient as the mesh is adapted.

#### 4. Dynamic re-meshing methods

In the previous section we have shown that static regridding methods are effective in computing the solution, but they are somewhat inefficient and require a rather large number of mesh points to be effective. It is reasonable to ask whether comparable accuracy can be obtained with a smaller number (indeed a fixed number) of mesh points if they are suitably placed. This is the philosophy behind methods which attempt to retain an error within a prescribed accuracy by optimally placing a fixed number of points. A review of these is given in [11]. An immediate indication that this approach is unlikely to succeed for (1.1) is given by the previous calculation of the number of points required to resolve the peak. If  $\|L^{-1}\|_{\infty}$  were bounded then it would be appropriate to take  $q = 4$  in our calculations and (3.7) would predict that the peak could then be resolved with a fixed number of points. However, the unboundedness of  $\|L^{-1}\|_{\infty}$  forces us to take  $q = 8$  leading to a need for an unbounded number of mesh points to achieve a consistent level of accuracy.

Now suppose that we consider a more general dynamic refinement method. Such methods are often based upon the idea of equidistributing a monitor  $M$  of the solution (such as the arc-length) which is large when the solution is changing rapidly. For the method described in Section 3 this implies that

$$\int_{r_i}^{r_{i+1}} M \, dr = \frac{1}{N} \int_0^1 M \, dr.$$

This equation for the mesh is then solved simultaneously with the underlying equation.

We consider first the commonly used arc-length monitor  $M = \sqrt{1 + u_x^2}$ . Using the approximation (2.2) for  $u$  we see that  $u_x$  dominates 1 within the peak and thus

$$\int_{r_i}^{r_{i+1}} M \, dr \approx u(r_{i+1}) - u(r_i).$$

Using (2.2) we then have (after some manipulation)

$$r_i \approx \frac{1}{\|u\|_{\infty}^2} \sqrt{\frac{3}{1 - i/N}} - 3,$$

which then gives

$$h_i \equiv r_{i+1} - r_i \approx \frac{1}{\|u\|_{\infty}^2} \sqrt{\frac{3}{2(i+1)N}}, \quad h_0 \approx \frac{1}{\|u\|_{\infty}^2} \sqrt{\frac{3}{2N}}.$$

The value of  $h_0$  thus scales in a very similar manner to the value obtained for the static regridding method when  $q = 4$ . The dynamic re-meshing method will therefore behave similarly, and in particular

will admit spurious solutions when  $\lambda = \lambda_0$ . Calculations with other monitor functions such as  $M = a + bu^p$  again give similar meshes to the above, with closely related errors. Essentially, this is because the singularity in (2.2) has a natural length scale of  $1/\|u\|_\infty^2$  and the dynamic meshing methods tend to place mesh points equally with respect to this. Unfortunately as we have shown, the mesh points need to be placed more closely as  $\|u\|_\infty$  increases in order to obtain accurate results. Numerical calculations (not presented here) all corroborate the above results.

## 5. Conclusions

We have shown that the special features of problem (1.1) require careful error estimates which take into account the growth in the norm of  $\|L^{-1}\|_\infty$ . If this growth is not taken into account then the adaptive procedure will not necessarily give an accurate solution and will also admit spurious solutions. The error estimate derived using the bound for  $\|L^{-1}\|_\infty$  leads to a method which is effective for the calculations on the reduced problem in the sphere. The next stage in the continuation of this work is to apply this estimate to a static regriding method for the full three dimensional problem. In principle the error estimate should be just as effective, but computational difficulties are likely to arise owing to the large number of elements that are likely to be necessary for the computation. Similar techniques are likely to be necessary for computations on the large number of critical problems related to (1.1).

## Acknowledgements

We gratefully acknowledge the support of the EPSRC grants GR/H63456 and GR/J75258 and the EC HCM grant on Singularities and Interfaces in Partial Differential Equations.

## References

- [1] J.G. Blom and J.G. Verwer, VLUGR3: a vectorisable adaptive grid solver for PDEs in 3D. 1. Algorithmic aspects and applications, Numerical Mathematics Research Report NM-R9404, CWI, Amsterdam (1994).
- [2] H. Brezis, Elliptic equations with limiting Sobolev exponents—the impact of topology, *Comm. Pure Appl. Math.* 39 (1986) S17–S39.
- [3] H. Brezis and L. Nirenberg, Positive solutions of nonlinear elliptic equations involving critical Sobolev exponents, *Comm. Pure Appl. Math.* 36 (1983) 437–477.
- [4] H. Brezis and L.A. Peletier, Asymptotics for elliptic equations involving critical growth, in: *Partial Differential Equations and the Calculus of Variations*, Vol. I (Birkhäuser, 1989) 149–192.
- [5] F. Brezzi, J. Rappaz and P. Raviart, Finite dimensional approximations of nonlinear problems, Part 1, *Numer. Math.* 36 (1980) 1–25.
- [6] C. Budd, Semilinear elliptic equations with near critical growth rates, *Proc. Roy. Soc. Edinburgh Ser. A* 107 (1987) 249–270.
- [7] C.J. Budd and A.R. Humphries, Weak finite dimensional approximations of radial solutions of semi-linear elliptic PDEs with near critical exponents, CMAIA Research Report 96/13, University of Sussex (1996); *Asymptotic Anal.*, submitted.

- [8] C.J. Budd, A.R. Humphries and A.J. Wathen, The finite element approximation of semi-linear elliptic PDEs with critical exponents in the cube, CMAIA Research Report 96/24, University of Sussex (1996); *SIAM J. Sci. Comput.*, submitted.
- [9] S. Chandrasekhar, *An Introduction to the Study of Stellar Structure* (Dover, New York, 1957).
- [10] M. Dobrowolowski and R. Rannacher, Finite element methods for nonlinear elliptic systems of second order, *Math. Nachr.* 94 (1980) 155–172.
- [11] W. Huang, Y. Ren and R.D. Russell, Moving mesh methods based on partial differential equations, *J. Comput. Phys.* 112 (1994) 279–290.
- [12] A.R. Humphries, C.J. Budd and A.J. Wathen, Finite element method solutions for semi-linear elliptic PDEs with critical Sobolev exponents on non-spherical 3D domains, in: L.T. Magalhães, C. Rocha and L. Sanchez, eds., *Proc. International Conference on Differential Equations—Equadiff '95*, Lisbon (World Scientific, 1997).
- [13] J.C. Lopez-Marcos and J.M. Sanz-Serna, Stability and convergence in numerical analysis, III. Linear investigation of nonlinear stability, *IMA J. Numer. Anal.* 8 (1986) 71–84.
- [14] T. Murdoch and C.J. Budd, Convergent and spurious solutions of nonlinear elliptic equations, *IMA J. Numer. Anal.* 12 (1992) 365–386.
- [15] R. Schoen, Conformal deformation of a Riemannian metric to constant scalar curvature, *J. Differential Geom.* 20 (1984) 479–495.
- [16] R.A. Trompert and J.G. Verwer, A static-regridding method for two-dimensional parabolic partial differential equations, *Appl. Numer. Math.* 8 (1991) 65–90.
- [17] J.G. Verwer and R.A. Trompert, An adaptive-grid finite-difference method for time-dependent partial differential equations, in: D. Griffiths and G. Watson, eds., *Numerical Analysis 1991*, Research Notes in Mathematics 260 (Pitman, 1992).